Title: CRUSTAL FRACTURING FIELD AND PRESENCE OF FLUID AS REVEALED BY SEISMIC ANISOTROPY: CASE HISTORIES FROM SEISMOGENIC AREAS IN THE APENNINES (ITALY)

Short title: Seismic anisotropy in the Apennine crust

Corresponding Author: Marina Pastori

c/o Istituto Nazionale di Geofisica e Vulcanologia – Centro Nazionale Terremoti

Via di Vigna Murata, 605

00143 Roma, Italy

First Author: Marina Pastori[1,2] (marina.pastori@ingv.it)

Other Authors: Piccinini Davide[2] (davide.piccinini@ingv.it), Valoroso Luisa[2] (luisa.valoroso@ingv.it), Wuestefeld Andreas[3] (andy.wuestefeld@bristol.ac.uk), Zaccarelli Lucia[4] (zaccarelli@ipgp.fr), Bianco Francesca[2] (bianco@ov.ingv.it), Kendall Micheal[3] (gljmk@bristol.ac.uk), Di Bucci Daniela[5] (daniela.dibucci@protezionecivile.it), Margheriti Lucia[2] (lucia.margheriti@ingv.it), and Barchi Massimiliano R.[1] (mbarchi@unipg.it).

Other authors' affiliations: 1. Università degli Studi di Perugia (IT); 2. Istituto Nazionale di Geofisica e Vulcanologia (IT); 3. University of Bristol (UK); 4. Institut de Physique du Globe de Paris (FR); 5. Dipartimento della Protezione Civile (IT).

Abstract

An automatic analysis code, Anisomat+, was developed, tested and improved to calculate anisotropic parameters: fast polarization direction and delay time.

Anisomat+ was applied on data coming from three zones of the Apennines in Italy. For each area, anisotropic parameters have been interpreted to determine the fracture and stress field taking into account the geological and structural settings.

It was recognized that the averages of fast directions are NW-SE–oriented at all sites, in agreement with the orientation of maximum horizontal stress as well as with the strike of the main fault structures. The mean values of normalized delay time range from 0.005 s/km to 0.007 s/km and to 0.009 s/km, respectively for L'Aquila region, Alto Tiberina Fault area and

Val d'Agri basin, suggesting a 3-4% of crustal anisotropy. Moreover, for each area, the spatial distribution of anisotropic parameters is examined, and for L'Aquila 2009 seismic sequence also temporal distribution is discussed.

1. Introduction

In the Earth's crust, anisotropy may be caused by preferentially aligned joints or microcracks, by layered bedding in sedimentary formations, or by highly foliated metamorphic rocks. Crustal anisotropy resulting from aligned cracks can be used to determine the state of stress in the crust, since in many cases cracks are preferentially aligned and/or opened by the active stress field and oriented parallel to the direction of the maximum horizontal stress (S_{Hmax}). In tectonically active areas, such as near active fault systems and volcanoes, anisotropy can be used to look for changes in the preferred orientation of cracks that may indicate a rotation of the stress field.

Both seismic P- and S-waves may exhibit anisotropy and, for both, the anisotropy may appear as a (continuous) dependence of velocity upon the direction of propagation. For S-waves, it may also appear as a (discrete) dependence of velocity upon the direction of polarization. For a given direction of propagation in any homogeneous medium, only two polarization directions are allowed, with other polarizations decomposing trigonometrically into these two. Hence, shear waves naturally "split" into separate arrivals with these two polarizations; in optics this is called birefringence, in seismology shear wave splitting (Barton, 2006).

During the last decades, the study of seismic anisotropy has provided useful information for the interpretation and evaluation of the active crustal deformation and the stress field in the light of two anisotropic interpretative models, proposed by Zinke and Zoback (2000), Crampin (1993) and Zatsepin and Crampin (1995), that will be described in the following sections. Shear wave splitting analysis can yield valuable information on upper crustal structure, fracture field, and presence of fluid-saturated rocks, being strictly related to stress-aligned, fluid-filled micro-cracks (Crampin, 1984; Barkved et al., 2004).

The automatic analysis code, Anisomat+, was developed to calculate anisotropic parameters, fast polarization direction (φ) and delay time (δt), and it has been compared with other two automatic analysis codes: Splitting Parameters Yield (SPY; Bianco and Zaccarelli, 2009) and

Shear Birefringence Analysis (SHEBA; Wuestefeld et al., 2010). It was observed that, if the number of measures is large enough, at each station the average values of the anisotropic parameters are comparable.

This work is aimed at constraining the crustal stress field and at providing information about the presence and migration of fluids in three different sites of the Apennines: Val d'Agri basin, Alto Tiberina Fault area and L'Aquila region. According to many investigators, the crack alignment is generated by the active stress field, and the knowledge of crustal anisotropic parameters can improve the understanding of the stress field perturbations and their effects on the seismogenic structures. In turn, this can contribute to understand the mechanisms that cause the seismogenic process: one of the primary goals of the geophysical research.

2. Seismic anisotropy and its relation with the crustal stress field and the presence of fluids

Seismic anisotropy is a commonly observed property of the Earth's crust (e.g. Crampin and Chastin, 2003, and references therein) and it can be quantified by the shear wave splitting, the elastic equivalent of the birefringence phenomenon in optics. When a seismic shear wave travels through an elastically anisotropic medium, its energy is split into two orthogonally polarized components that travel at different velocities. The polarization direction of the fastest wave is called fast direction (φ) and the lag of the slower wave is the delay time (δt).

There are at least two main interpretations for the shear wave splitting in the crust (Crampin and Lovell, 1991): (i) the intrinsic structural fabric due to aligned macroscopic fractures (inherited from ancient tectonic phases) or aligned anisotropic minerals (the latter generally found in metamorphic lithotypes, where they can cause rock foliation, Brocher and Christensen, 1990); or (ii) the presence of fluid-saturated micro-cracks or fractures, aligned or opened by the active stress field (Crampin, 1993).

In the (i) case (Figure 1a), φ is parallel to the strike of the fractures or of the mineral alignment, thus it is not related to the active stress field, and δt measures the fabric strength (Zinke and Zoback, 2000). In the (ii) case (Figure 1b), φ is typically polarized parallel to the direction of the maximum horizontal stress, as suggested by the Extensive-Dilatancy Anisotropy model (EDA; Crampin, 1978), δt is a measure of the intensity and/or thickness of the fractures field that would be sensitive to local variations of the stress field (e.g. variations related to the

seismic cycle). In this last interpretation, the dominant fracture direction, the crack density and therefore the maximum horizontal stress direction can be estimated from anisotropic parameters.

The three selected areas are located along the Italian Apennines, a fold-and-thrust belt formed by a deformed sedimentary cover overlying a crystalline crustal basement; this suggests that the anisotropy may be interpreted as principally caused by fractures or microfractures alignment.

In this work, we take into account some interpretative models available in the literature. Zinke and Zoback (2000) proposed a theory for which the local strain field and cracks alignments are the sum of present and previous tectonics phases and are not necessarily related to the active stress; therefore the anisotropic parameters variations are thus only space-dependent. Differently, the Extensive Dilatancy Anisotropy model (Crampin, 1993) and its development in Anisotropic Poro Elasticity model (APE; Zatsepin and Crampin, 1995) propose that fluid-filled micro-cracks are the main responsible for anisotropy and are aligned or 'opened' by the active stress field; the local variations of the stress field might be therefore related to the evolution of the pore pressure in time. In this case, the variations of the anisotropic parameters are both space- and time- dependent. Following these latter theories and in accordance with Crampin and Gao (2010), monitoring anisotropic parameter variations could be a potential tool for earthquakes forecasting. These investigators consider the anisotropic parameters sensitive to the variations of the stress field related to both the earthquake occurrence and the variations of fluid pressure in the rock volume.

3. Anisomat+: developing, testing and validating

Our first objective for this work has been to develop a semi-automatic code able to evaluate the anisotropic parameters, fast direction polarization (φ) and delay time (δt), and then to apply it to the crustal earthquakes located in selected test areas, aimed at characterizing the fracture field of the crust and/or the microfracture field and consequently the stress field. In literature many different techniques are proposed to calculate the anisotropic parameters, and all of them present weaknesses as well as strength points (Silver and Chan, 1991; Zhang and Schwartz, 1994; Crampin and Gao, 2006; Margheriti et al., 2006).

Elaborating a large amount of data in a very short time is the primary advantage in utilizing an automatic code; in this way, generally, the errors due to the subjectivity are reduced, even

though the accuracy and robustness of each single elaboration may be affected by some bias. The main goal of this automation has been to minimize the operator intervention during the analysis and to allow the analysis of waveforms just as they are stored in the Italian Seismic Network archive (http://iside.rm.ingv.it). The rationale behind this choice is that this code will be useful in the real-time monitoring.

"Anisomat+" is a set of MatLab scripts able to retrieve crustal anisotropy parameters from three-component seismic recording of local earthquakes. The code uses the waveform cross-correlation method on the horizontal components of the seismograms allowing measuring the similarity of the pulse shape between two S waves. These two waves have similar shape, mutually orthogonal oscillation directions and travel with different velocities. The analysis procedure consists in choosing the appropriate frequency range that better highlights the signal containing the shear waves, and a time window for the analysis on the seismograms centred on the S arrival (the temporal window contains at least one cycle of S waves).

To ensure the use of an appropriate waveform, Anisomat+ applies quality controls on: 1) the geometrical incidence angle measured from the vertical, which ranges between 0° and 45°; 2) the S-wave picking uncertainty; 3) the ratio between the amplitude of horizontal and vertical components ($A_{N\text{-}S\ E\text{-}W}/A_Z>1.5$); 4) the signal to noise ratio (rmss./rmsp > 4).

The selection criteria applied on the data guarantee that shear wave energy mainly concentrates in the horizontal plane. If the controls are passed, Anisomat+ determines the fast polarization direction and delay time values by using the cross-correlation function. Thus, we can get shear wave splitting parameters by rotating (with steps of 1°) the N and the E components and calculating their cross-correlation coefficient: when the absolute value of cross-correlation coefficient takes the maximum value, we regard the rotation direction as the fast-wave direction and the amount of the lag time as the delay time of the slow-wave to the fast-wave.

Figure 2 shows an example of the graphic output of Anisomat+ elaboration where horizontal overlap of the fast and slow components, temporal variation of polarization vectors and particle motion before and after delay time correction are shown.

To verify if the automatic analysis code works properly we made several tests. The first step was to compare the results from the automatic versions of Anisomat+ to those obtained by the same code applied manually (Pastori et al., 2009). Then, in a second step we compared Anisomat+ with a semi-automatic code called Splitting Parameters Yield (SPY; Bianco and Zaccarelli, 2009), based on a different technique and independently developed under MatLab.

In both cases, the comparison was carried out on the same dataset recorded in the Val d'Agri basin in Southern Italy. As third step, to confirm the robustness of our semiautomatic code, we compared Anisomat+ to Shear Birefringence Analysis (SHEBA), an additional automatic code developed by the University of Bristol team to estimate anisotropic parameters automatically (Wuestefeld et al., 2010). In this final comparison we used the dataset recorded in the Alto Tiberina Fault area in Central Italy.

In general, the comparison between Anisomat+ and the other codes (Anisomat manual version, SPY and SHEBA; Figure 3) gave consistent results. It is possible to observe that the total results for both fast polarization directions and magnitude of the delay times is very similar, although, looking at single station results, one could find from slight to strong differences.

In the comparisons made, we tried to use the same input parameters (filter, window length, etc) taking into account that each code uses different initial conditions and computational methods (covariance matrix, cross-correlation or both). Moreover, each of them was developed to analyse a specific type of data (volcanic seismicity for SPY, well data for SHEBA and shallow and deep seismic events of tectonic nature for Anisomat+). These differences in the codes are the reason for different single results; however, if the number of measures is large enough, the average values of the parameters are comparable.

4. Case histories from three seismogenic areas along the Apennine chain

The Apennine chain represents the frame of the Italian peninsula and is traditionally divided into three parts: Northern, Central and Southern Apennines. This mountain chain is a fold-and-thrust belt whose core is currently affected by SW-NE active extension, as shown by breakout data and seismicity (Montone et al., 2004), as well as by geological and geomorphological analyses (e.g., Galadini, 1999; D'Agostino et al., 2001). This extension is perpendicular to the main active and inherited faults; moreover the normal faulting can be accompanied by oblique fault slip (e.g. Piccardi et al., 2006 and references therein). According with some investigators (i.e., Di Bucci and Mazzoli, 2002 for a discussion), the outer belt is instead still undergoing shortening (e.g. Boncio and Bracone, 2009; Boccaletti et al., 2010).

For each part of the thrust belt, we selected a study area containing an intramountain extensional basin filled by Quaternary continental deposits and located at the top of the Apennine thrust sheets, which are mainly composed of marine sedimentary successions. For each study area, we defined the dominant fast direction and the delay time. The results were

then interpreted in the light of the geological and structural setting. It was recognized that the average of fast directions is oriented NW-SE at all sites, in agreement with the orientation of the strike of the main fault structures and also with the active stress field (based on stress indicators as focal mechanisms, e.g. Cucci et al., 2004, Boncio et al., 2004 and Chiaraluce et al., 2007, and borehole breakouts, e.g Mariucci et al., 2008; 2010; Figure 4). The space variations of the delay time magnitude are used to define where the anisotropic medium is confined.

4.1. Case 1: Val d'Agri basin

The Val d'Agri area, in the Southern Apennines, has attracted the attention of geoscientists over the past two decades. The presence of oil fields ranking as the largest in onshore Europe, and the high seismogenic potential documented by historical earthquakes motivated geophysical investigations that focus on the subsurface structure and seismotectonics (Borraccini et al., 2002; Cucci et al., 2004; Shiner et al., 2004; Pastori et al., 2009, Valoroso et al., 2009). Nonetheless, there is still an open discussion about the location of the seismogenic source of a M 7.0 earthquake occurred in that area in 1857 (Burrato and Valensise, 2008, and references therein). Here, we investigated the upper crust of the Val d'Agri, trying to relate the anisotropy to the active structures and the stress field.

Figure 5 shows the frequency diagrams of the fast polarization directions at stations having more than 10 measurements. The length of rose petals is proportional to the number of measurements in the correspondent 10° interval. The lower inset shows the total fast directions at all stations.

We notice a NW–SE dominant fast direction at most of the stations (AG04, AG09, AG13, AG14, AG18) whereas other measurements are slightly rotated in a more N100°E direction (AG11 and AG17) or strike E–W (AG05). The remaining station, AG01, does not show a preferential orientation, but the major petals display strikes coherent with the other results. As a whole, in Val d'Agri we observe a dominant fast polarization direction striking NW–SE, perpendicular to the current S_{hmin} in the region as obtained from available active stress indicators such as borehole breakout and T-axis of focal mechanisms (Cucci et al. 2004). Our findings also agree with the recent finding of a NW-trending normal faulting mechanism, obtained by Valoroso et al. (2009) by using the same dataset.

For the region we estimated an average normalized delay times of 0.009 s km^{-1}. The estimated values for single stations may vary strongly, ranging from 0.002 to 0.012 s km^{-1}. We found greater values (> 0.01 s km^{-1}; stations AG09, AG14, AG18) at stations located

along the SW margin of the Val d'Agri basin, whereas lower values (below 0.01 s km^{-1}) characterize both the sites AG04 and AG11, along the NE margin of the basin, and the station AG05, located to the SE of the nearby Vallo di Diano basin. This is shown by the colours in Figure 5, which represent the interpolated values of normalized delay times.

4.2. Case 2: Alto Tiberina Fault area

In the Northern Apennines, the Upper Tiber River Valley hosts an important geological structure, called Alto Tiberina Fault (hereinafter ATF). Defined in literature as a Low Angle Normal Fault (LANF; e.g. Boncio et al., 2000; Collettini and Barchi, 2002), it attracted the attention of the investigators since the end of the nineties as an important tectonic structure both for the accommodation of significant amounts of structural extension and in terms of seismic hazard.

The ATF geometry is well known from a structural point of view (Barchi et al., 1998; Chiaraluce et al., 2007, Mirabella et al., 2008); moreover, in the same area, earthquakes with hypocenters down to 30 km were recorded during the so-called "Città di Castello experiment" and preliminarily localized by Piccinini et al. (2003). Geological and seismological data show that the ATF is an active fault system that separates a seismically active hanging wall block from an aseismic footwall. In the hanging wall, minor synthetic and antithetic high-angle normal faults root down into the ATF, which acts as a detachment, suggesting the simultaneous activity of the whole normal fault system. The high-angle normal faults in the ATF hanging wall slip seismically, generating both microseismicity and moderate magnitude earthquakes ($5<M<6$) such as the 1984 Gubbio main shock (Chiaraluce et al., 2007). This allows us to characterize the anisotropic behaviour of a rock volume above and below the ATF by computing the anisotropic parameters. We are also able to compare the characteristics of the earthquakes related to the ATF activity from those related to the high angle normal faults. This information is relevant when assessing detailed seismic hazard and accurately constraining possible ground shaking scenarios.

Figure 6 shows the rose diagrams of the fast polarization directions at stations having more than 10 measurements. In the total fast plot (Figure 6, upper inset) we observe a dominant NW-SE direction, i.e. the same orientation of the major faults exposed in the area (redrawn from Mariucci et al., 2008). This direction is also perpendicular to the S_{hmin} of the active extensional stress field (Boncio and Lavecchia, 2000).

In detail, the means of fast directions, at the selected 13 stations, are roughly parallel to the main geological structures, even if there are stations with rotated directions (i.e. C002, B4, B5, A003). If we consider only normalized delay times (shadowed area in Figure 6), we

observe higher values, 0.01 s/km, located at stations C3 and C004, both located in the footwall of the Gubbio Fault and where most of the seismicity occurs. These values suggest a percentage of anisotropy A=3% ($A=V_{Smean}*\delta tn*100$, Wuestefeld et al., 2010; V_{Smean} is assumed 3.3 km/s according to Piccinini et al., 2003).

4.3. Case 3: L'Aquila region

The 2009 L'Aquila seismic sequence gave us the opportunity to study the shear-wave splitting in the region where a M_w>6 earthquake (Scognamiglio et al., 2010, Pondrelli et al., 2010) occurred on April 6th 2009. According to some authors (Gao and Crampin, 2003; 2006; Crampin and Gao, 2010), observations of shear-wave splitting at seismic stations located just above a seismic sequence before and after the occurrence of a mainshock, might suggest that the time-delays and fast directions of split shear-waves could provide a tool to monitor the stress build-up before an earthquake and the stress release as the earthquake occurs.

The L'Aquila sequence occurred in a recently silent, yet very seismic region of the extensional belt along the Central Apennines. The seismic sequence started at the beginning of 2009 and was confined within the upper 10–15 km of the crust (Chiarabba et al., 2009). We analysed the shear wave splitting resulting from data acquired by three stations of the Italian Seismic National Network (AQU, CAMP and FAGN), during one year from 1st January 2009 to 31th December 2009. The results were compared to the stress field and structural indicators of the area and some hypotheses were discussed on the correspondence between temporal changes in anisotropic parameters and the evolution of the seismic sequence.

In Figure 7 the rose diagrams and the means (according to the Von Mises criterion; Mardia, 1972) of fast direction polarization (blue lines) are shown; in the lower inset, the fast directions cumulated for all stations are plotted. The fast directions are mainly WNW-ESE-oriented, about N122°, well in agreement with the S_{hmin} (Boncio et al., 2004; Mariucci et al., 2010; Pondrelli et al., 2010), except for station FAGN, where a SSW-NNE fast direction (about 28°) was found. This direction, which markedly differs from the general structural setting (EMERGEO Working Group, 2010), may be related to the presence of peculiar seismic wavefields at station FAGN (Calderoni et al., 2010).

The delay time values follow the same pattern shown by the fast directions, that is, they are similar each other at AQU and CAMP stations (about 0.005 s/km), whilst a higher value (0.007 s/km) is found at FAGN station.

Looking at changes of anisotropic parameters in time, in particular while approaching the mainshock, we observe some variations of the seismic wave propagation properties. Fluid over-pressurization in fault structures has been suggested as a primary trigger of normal

faulting earthquakes (Sibson, 2000; Chiodini et al., 2004). In the only Italian case occurred in recent times and comparable to the L'Aquila sequence (i.e., the 1997 Umbria-Marche sequence), there is evidence for a major role played by fluids over the seismicity (Chiarabba et al., 2009; Miller et al., 2004). From the a posteriori analysis of the temporal variations of anisotropic parameters (Figure 8) we observed an overall increase of the delay time (likely due to an increase of the aligned fractures) and a 90°-flips of some of the fast directions (likely due to over-pressured fluids) starting before the 6th April mainshock. The same trend of δt is observed around Julian days 170-180 (end of June 2009); in this period, a seismic sequence started to the NW of CAMP station. These a posteriori observations, which are quite scattered, are consistent with a possible complex sequence of dilatancy-diffusion processes taking place in the rock volume where the earthquake was preparing and the seismic sequence occurring. This may imply that fluids played a key role in the fault failure process and in the development of the seismic sequence, as hypothesized by Lucente et al. (2010) for the foreshock sequence.

5. Conclusions

In this work we analyzed several thousands of waveforms, recorded at more than 50 stations, getting about one thousand anisotropic measurements in terms of fast direction and delay time from the three studied areas of the Apennines: Val d'Agri basin, Alto Tiberina Fault area and L'Aquila region.

Overall the obtained results show that average anisotropic parameters are robust measurements: NW-SE average fast directions and average normalized delay times ranging from 0.05 s/km to 0.09 s/km were found (Figure 4). The mean values of normalized delay time range from 0.005 s/km to 0.007 s/km and to 0.009 s/km, respectively for L'Aquila region, Alto Tiberina Fault area and Val D'Agri basin, suggesting a 3-4% of crustal anisotropy; this same percentage found by Piccinini et al. (2006) in Central Italy by studying the 1997 Umbria-Marche seismic sequence. This percentage of differential shear wave anisotropy testifies (in the EDA frame interpretation) a crack density $\varepsilon = 0.045$ ($\varepsilon = N\alpha 3/\nu$, where N is the number of cracks of radius α in volume ν), the critical crack density at which nearby cracks begin to coalesce to form through-going fractures (Crampin, 1993).

These values can be related to different causes, such as the active stress field and the pre-existing crustal structures and tectonic style. Moreover, they provide information about the presence and migration of fluids at depth.

In each area we found a close correspondence between the average fast polarization direction and the orientation of the minimum horizontal stress (Figure 4), as suggested by the EDA model proposed by Crampin (1993). However, the NW-SE direction found along the Apennines is also the strike of the main pre-existing geological structures (both compressional and extensional); therefore, the observed anisotropy may also have been driven by the inherited fracture fields, following the interpretation proposed by Zinke and Zoback (2000). A connection between the temporal variations of the anisotropic parameters and the possible stress changes (in term of pore-pressure changes, stress and fracture field variation, fluid migration, etc.) related to the L'Aquila mainshock and the associated seismic sequence was however observed, and these variations are compatible with those predicted by APE model. Therefore, the observed temporal variation of anisotropic parameters suggests that the anisotropic results are related to the active stress field and its possible perturbations, and that they could be better interpreted following the EDA-APE model.

Since this technique was applied in areas where earthquakes occur, and therefore where faulting process has produced fractures, it is difficult to separate the contributions to anisotropy of fractures and microfractures.

These areas, in fact, are affected by an extensional tectonic regime where the strike of the active faults is parallel to that of the maximum horizontal stress, and where the cracks opening (that records the active stress field during an earthquake) increases as well the fracturing degree of the rock mass, making it difficult to discriminate which process is more relevant.

To conclude, we think that a systematic study of the spatial and temporal variations of anisotropic parameters at stations distributed over the Italian territory could provide a new key for the understanding of the seismogenic process, even in view of their future, possible application as warnings for strong earthquakes.

Acknowledgments - This paper is part of Marina Pastori Ph.D. thesis and was presented at 29° GNGTS meeting (Prato, 26-28 October 2010), where it was acknowledged with the Licio Cernobori award bestowed by the AGLC. We would like to thank all the INGV's researchers who contributed to make available the seismic datasets analyzed.

We are grateful to the Guest Editor of the Bollettino di Geofisica Applicata e Teorica Giuliana Rossi, Andrea Argnani for his thorough review and the anonymous reviewer.

References

Barchi M., DeFeyter A., Magnani B., Minelli G., Pialli G., Sotera B.; 1998: *The structural style of the Umbria–Marche fold and thrust belt*. Memorie della Società Geologica Italiana, **52**, 557–578.

Barton, N.; 2006: *Rock quality, seismic velocity, attenuation and anisotropy.* Taylor & Francis, 729 pp.

Barkved O., Bartman B., Gaiser J., Van Dok R., Johns T., Kristiansen P., Probert T., Thompson M.; 2004: *The many facets of multicomponent seismic data*. Oilfield Rev. Summer, 42-56, Schkumberger.

Bianco F. and Zaccarelli L.; 2009: *A reappraisal of shear wave splitting parameters from Italian active volcanic areas through a semiautomatic algorithm*. Journal of Seismology, **13(2)**, 253-266.

Boccaletti M., Corti G. and Martelli L.; 2010: *Recent and active tectonics of the external zone of the Northern Apennines (Italy)*. Int. J. Earth Sci. (Geol. Rundsch.), doi: 10.1007/s00531-010-0545-y.

Boncio P., Brozzetti F. and Lavecchia G.; 2000: Architecture and seismotectonics of a regional low-angle normal fault zone in central Italy. Tectonics, 19, 1038–1055.

Boncio P. and Lavecchia G.; 2000: A geological model for the Colfiorito earthquakes *(September–October 1997, central Italy)*. Journal of Seismology, **4**, 345–356.

Boncio P., Lavecchia G. and Pace B.; 2004: *Defining a model of 3D seismogenic sources for Seismic Hazard Assessment applications: the case of central Apennines (Italy)*. J. Seismol., **8**, 407–425.

Boncio P. and Bracone V.; 2009: *Active stress from earthquake focal mechanisms along the Padan-Adriatic side of the Northern Apennines (Italy), with considerations on stress magnitudes and pore-fluid pressures.* Tectonophysics, **476**, 180-194.

Borraccini F., De Donatis M., Di Bucci D. and Mazzoli S.; 2002: *3D Model of the active extensional fault system of the high Agri River valley, Southern Apennines, Italy*. In: Jessell M. W. (Ed.) – General contributions 2002. Journal of the Virtual Explorer, **6**, 1-8 pp.

Brocher T.M. and Christensen N.I.; 1990: *Seismic anisotropy due to preferred mineral orientation observed in shallow crustal rocks in southern Alaska*. Geology (Boulder), **18**(8), 737-740.

Burrato P. and Valensise G.; 2008: *Rise and fall of a hypothesized seismic gap: source complexity in the Mw=7.0 16 December 1857 Southern Italy Earthquake*. BSSA, **98**(1),

139-148.

Calderoni G., Rovelli A. and Di Giovambattista R.; 2010: *Large amplitude variations recorded by an on-fault seismological station during L'Aquila earthquakes: Evidence for a complex fault-induced site effect*. Geophisical Research Letters, **37**, L24305, 5 pp.

Chiarabba C., Amato A., Anselmi M., Baccheschi P., Bianchi I., Cattaneo M., Cecere G., Chiaraluce L., Ciaccio M.G., De Gori P., De Luca G., Di Bona M., Di Stefano R., Faenza L., Govoni A., Improta L., Lucente F.P., Marchetti A., Margheriti L., Mele F., Michelini A. Monachesi G., Moretti M., Pastori M., Piana Agostinetti N., Piccinini D., Roselli P., Seccia D. and Valoroso L.; 2009: *The 2009 L'Aquila (central Italy) M_W6.3 earthquake: Main shock and aftershocks*. Geophys. Res. Lett., **36**(18), L18308, 6 pp, doi:10.1029/2009GL039627.

Chiaraluce L., Chiarabba C., Collettini C., Piccinini D. and Cocco M.; 2007: *Architecture and mechanics of an active low-angle normal fault: Alto Tiberina Fault, northern Apennines, Italy*. Journal of Geophysical Research, **112**, B10310, doi:10.1029/2007JB005015.

Chiodini G., Cardellini C., Amato A., Boschi E., Caliro S., Frondini F. and Ventura G.; 2004: *Carbon dioxide Earth degassing and seismogenesis in central and southern Italy*. Geophys. Res. Lett., **31**, L07615, 4 pp.

Collettini C. and Barchi M.R.; 2002: *A low angle normal fault in the Umbria region (Central Italy): a mechanical model for the related micro- seismicity*. Tectonophysics, **359**, 97–115.

Crampin S.; 1978: *Seismic wave propagation through a cracked solid: polarization as a possible dilatancy diagnostic*. Geophys J R Astron Soc, **53**, 467–496.

Crampin S.; 1984: *Effective anisotropic elastic-constants for wave propagation through cracked solids*. Geophys J R Astron Soc., **76**, 135–145.

Crampin S.; 1993: *Arguments for EDA.* Canadian Journal of Exploration Geophysics, 29(1), 18-30.

Crampin S. and Chastin S.; 2003: *A review of shear-wave splitting in the crack-critical crust*. Geophys J. Int., **155**, 221- 240.

Crampin S. and Gao Y.; 2010: *Earthquakes can be stress-forecast*. Geophysical Journal International, **180**, 1124-1127.

Crampin S. and Gao Y.; 2006: *A review of techniques for measuring shear wave splitting above small earthquakes*, Physics of the Earth and Planetary Interiors, **59**(1-2), 1-14.

Crampin S. and Lovell J.H.; 1991: *A decade of shear-wave splitting in the Earth's crust: what does it mean? what use can we make of it? and what should we do next?* Geophys J. Int., **107**, 387-407.

Cucci L., Pondrelli S., Frepoli A., Mariucci M.T. and Moro M.; 2004: *Local pattern of stress field and seismogenic sources in Melandro Pergola basin and in Agri valley (Southern Italy)*. Geophys. J. Int., **156**, 575-583.

D'Agostino N., Jackson J.A., Dramis F. and Funiciello, R.; 2001: *Interactions between mantle upwelling, drainage evolution and active normal faulting: An example from the central Apennines (Italy)*. Geophysical Journal International, **147**, 75–497, doi: 10.1046/j.1365-246X.2001.00539.x.

Di Bucci D. and Mazzoli S.; 2002: *Active tectonics of the Northern Apennines and Adria geodynamics: new data and a discussion*. J. Geodyn., **42**, 687–707.

Emergeo Working Group; 2010: *Evidence for surface rupture associated with the Mw 6.3 L'Aquila earthquake sequence of April 2009 (central Italy)*. Terra Nova, **22**, 43–51.

Galadini F.; 1999: *Pleistocene changes in the central Apennine fault kinematics: A key to decipher active tectonics in central Italy*. Tectonics, **18**(5), 877–894, doi: 10.1029/1999TC900020.

Gao Y. and Crampin S.; 2003: *Temporal variations of shear- wave splitting in field and laboratory studies in China*. Spec. Issue J Appl Geophys., **54**, 279–287.

Gao Y. and Crampin S.; 2006: *A stress-forecast earthquake (with hindsight), where migration of source earthquakes causes anomalies in shear-wave polarisations*. Tectonophysics, **426**(3-4), 253-262.

Lucente F.P., De Gori P., Margheriti L., Piccinini D., Di Bona M., Chiarabba C. and Piana Agostinetti N.; 2010: *Temporal variation of seismic velocity and anisotropy before the 2009 M_w 6.3 L'Aquila earthquake, Italy*. Geology, **38**(11), 1015-1018.

Mardia, K.V.; 1972: *Statistic of directional data*. Academic Press, New York and London.

Margheriti, L., Ferulano, M.F. & Di Bona, M., 2006. *Seismic anisotropy and its relation with crust structure and stress field in the Reggio Emilia region (Northern Italy),* Geophys. J. Int., **167**(2), 1035–1045.

Mariucci M.R., Montone P., Pierdominici S.; 2008: *Active stress field in central Italy: a revision of deep well data in the Umbria region*. Annals of Geophysics, **51**(2-3), 433-442.

Mariucci M.A, Montone P. and Pierdominici S.; 2010: *Present-day stress in the surroundings of 2009 L'Aquila seismic sequence (Italy)*. Geophys. J. Int., **182**, 1096–1102 doi:

10.1111/j.1365-246X.2010.04679.x.

Miller S.A., Collettini C., Chiaraluce L., Cocco M., Barchi M.R. and Kraus J.B.; 2004: *Aftershocks driven by a high-pressure CO2 source at depth*. Nature, **427**, 724–727.

Mirabella F., Barchi M.R. and Lupattelli A.; 2008: *Seismic reflection data in the Umbria-Marche region; limits and capabilities to unravel the subsurface structure in a seismically active area.* Annals of Geophysics, **51(**2-3), 383-396.

Montone P., Mariucci M.T., Pondrelli S., Amato A.; 2004: *An improved stress map for Italy and surrounding regions (central Mediterranean)*. J. Geophys. Res., **109**(B10410), 22 pp., doi:10.1029/2003JB002703.

Pastori M., Piccinini D., Margheriti L., Improta L., Valoroso L., Chiaraluce L. and Chiarabba C.; 2009: *Stress aligned cracks in the upper crust of the Val d'Agri region as revealed by shear wave splitting*. Geophys. J. Int., **179**, 601–614.

Piccardi L., Tondi G. and Cello G.; 2006: *Geo-structural evidence for active oblique estension in South-Central Italy.* In: Pinter N., Grenerczy G., Weber J., Stein S., Medak D. (eds), The Adria microplate: GPS geodesy, tectonics and Hazard. NATO Science Series IV-Earth and Environmental Sciences, Springer, **61**., 95-108.

Piccinini D., Cattaneo M., Chiarabba C., Chiaraluce L., De Martin M., Di Bona M., Moretti M., Selvaggi G., Augliera P., Spallarossa D., Ferretti G., Michelini A., Govoni A., Di Bartolomeo P., Romanelli M., Fabbri J.; 2003: *A microseismic study in a low seismicity area of Italy: the Città di Castello 2000–2001 experiment*. Ann. Geophys., **46**(6), 1315–1324.

Piccinini D., Margheriti M., Chiaraluce L. and Cocco M.; 2006: *Space and time variation of crustal anisotropy during the 1997 Umbria-Marche, central Italy, seismic sequence.* Geophysical Journal International, **167(**3), 1482-1490.

Pondrelli S., Salimbeni S., Morelli A., Ekström G., Olivieri M. and Boschi E.; 2010: *Seismic moment tensors of the April 2009, L'Aquila (Central Italy), earthquake sequence*. Geophys. J. Int., **180**, 238–242, doi: 10.1111/j.1365-246X.2009.04418.x.

Scognamiglio L., Tinti E., Michelini A., Dreger D.S., Cirella A., Cocco M., Mazza S. and Piatanesi A.; 2010: *Fast determination of moment tensors and rupture history; what has been learned from the 6 April 2009 L'Aquila earthquake sequence*. Seismological Research Letters, **81(**6), 892-906.

Shiner P., Beccacini A. and Mazzoli S.; 2004: *Thin-skinned versus thick- skinned structural models for Apulian carbonate reservoirs; constraints from the Val d'Agri fields, S Apennines, Italy*. Mar Petrol Geol, **121**(7), 805–827.

Sibson R.H.; 2000: *Tectonic controls on maximum sustainable overpressure; fluid redistribution from stress transitions.* Journal of Geochemical Exploration, **69-70**, 471-475.

Silver P.G. and Chan W.W.; 1991: *Shear wave splitting and subcontinental mantle deformation*. Journal of Geophysical Research, **96(**B10), 16.429-16.454.

Valoroso L., Improta L., Chiaraluce L., Di Stefano R., Ferranti L., Govoni A. and Chiarabba C.; 2009: *Active faults and induced seismicity in the Val d'Agri area (Southern Apennines, Italy)*. Geophys J Int, **178**(1), 488–502.

Wuestefeld A., Al-Harrasi O., Verdon J.P., Wookey J. and Kendall J.M.; 2010: *A strategy for automated analysis of passive microseismic data to image seismic anisotropy and fracture characteristics*. Geophysical Prospecting, **58**, 755–773.

Zatsepin S.V. and Crampin S.; 1995: *Rock deformation; a non-linear anisotropic poro-elastic theory (APE) for pre-stressed fluid-saturated rock.* International Union of Geodesy and Geophysics, General Assembly, **21**, Week B, pp.340.

Zhang Z. and Schwartz S.Y.; 1994: *Seismic anisotropy in the shallow crust of the Loma Prieta segment of the San Andreas fault system.* Journal of Geophysical Research, **99**(B5), 9651-9661.

Zinke J.C. and Zoback M.D.; 2000: *Structure-related and stress-induced shear-wave velocity anisotropy; observations from microearthquakes near the Calaveras Fault in Central California.* Bulletin of the Seismological Society of America, **90**(5), 1305-1312.

CAPTIONS

Figure 1 – Main crustal sources of the shear wave splitting phenomena: **a)** aligned anisotropic minerals (mainly associated to metamorphic rocks); **b)** filled-fluid micro-cracks or fractures (mainly associated to sedimentary rocks).

Figure 2 – Example of the graphic output of Anisomat+ elaboration. The two top panels show the horizontal component rotated in the fast and slow reference system before and after the delay correction. The intermediate panel shows the polarization vectors of the same time window. The bottom panels show particle motion before and after the delay time correction.

Figure 3 – Schematic steps and parameters of analysis adopted for each comparison test. Anisomat+ was compared to Anisomat (manual version), Splitting Parameters Yield (SPY) and Shear Birefringence Analysis (SHEBA); the total results gave generally consistent results.

Figure 4 - Italian stress indicators (for legend details see World Stress Map Rel. 2008, *http://dc-app3-14.gfz-potsdam.de/pub/stress_data/stress_data_frame.html*), compared to the cumulated anisotropic results (average values of fast directions (black lines) and normalized delay times) obtained for each studied areas: ATF=0.007 s/km; AQU=0.005 s/km; VA=0.009 s/km. It is possible to recognise a close correspondence between fast directions and the maximum horizontal compressive stress (in agree with EDA model; Crampin, 1993)

Figure 5 – Rose diagrams of the fast polarization directions obtained for the Val d'Agri basin. The size of the roses on the map is proportional to the number of measurements. The bottom inset shows the total fast directions at all stations. The mean fast directions are almost orthogonal to the minimum horizontal stress (S_{hmin}) in the area, represented by the double-headed red arrow (Cucci et al., 2004). The coloured area corresponds to the variation of the normalized delay time.

Figure 6 - Results from the anisotropic elaboration (rose diagrams) shown along with earthquake localizations (blue dots) and main structural features of the Alto Tiberina Fault area (from Mariucci et al., 2008). The size of rose diagrams representing the polarization directions is proportional to the number of the measurements. Only the stations with more than 10 measurements are reported. The directions at each station, as well as the total of the measurements (upper inset), are almost perpendicular to the S_{hmin}, which strikes about NE-SW.

Spatial variation of normalized delay time, represented by the shadowed areas, and mean of fast directions (blue lines) are reported in the map. A comparison among mean fast direction,

minimum horizontal stress direction (Boncio and Lavecchia, 2000; Montone et al., 2004) and main geologic structures (Mariucci et al., 2008) shows a general consistence.

Figure 7 – Two different representations of the obtained anisotropic results for the L'Aquila area. 1) Fast direction rose diagrams, with petal size proportional to the number of the measurements, along with earthquake epicentres (yellow dots) and main structural features (red lineaments modified from EMERGEO Working group, 2010). 2) Mean fast directions (blue lines) scaled to the normalised delay time computed at each station. Exception made for station FAGN, the directions at the other stations and the total of the measurements (lower inset) are almost perpendicular to the S_{hmin}, which strikes about NE-SW.

Figure 8 – Temporal variation of the anisotropic parameters for the 2009 L'Aquila seismic sequence: A) delay time and B) fast direction for AQU station (see Figure 7). The large dots in A) represent individual measurements, whereas the line is the interpolation of the mean values (small dots) calculated over 5 measurements by using a sliding window. In B) the dashed lines represent the mean of the initial and Dominant Fast Direction (DFD) computed, respectively, before and after the mainshock (indicated by the star). A secondary direction is recognized after the mainshock, given by the 90°-flips from the mean of DFD and also visible in the two rose-diagrams. In the bottom inset, the total fast measurements are also shown; the two shadowed areas represent the standard deviation calculated for the mean values.

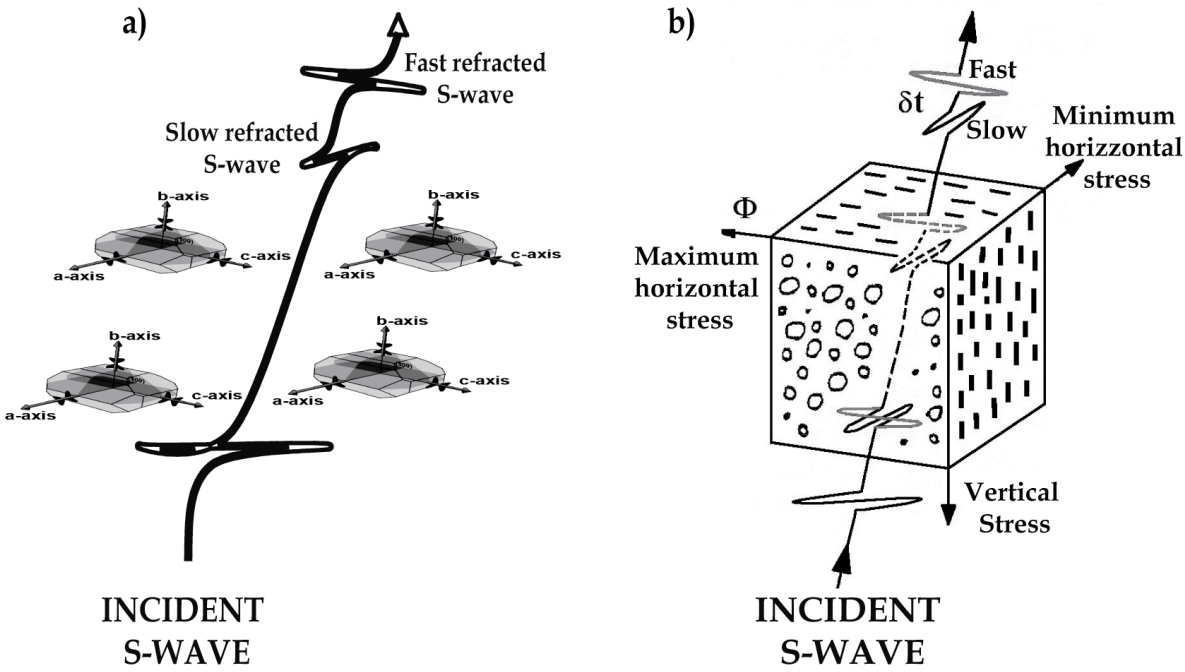
a)
Fast refracted
S-wave
Slow refracted
S-wave
b-axis
c-axis
a-axis
INCIDENT
S-WAVE
b)
Fast
δt
Slow
Minimum
horizzontal
stress
Φ
Maximum
horizontal
stress
Vertical
Stress
INCIDENT
S-WAVE

Figure 1

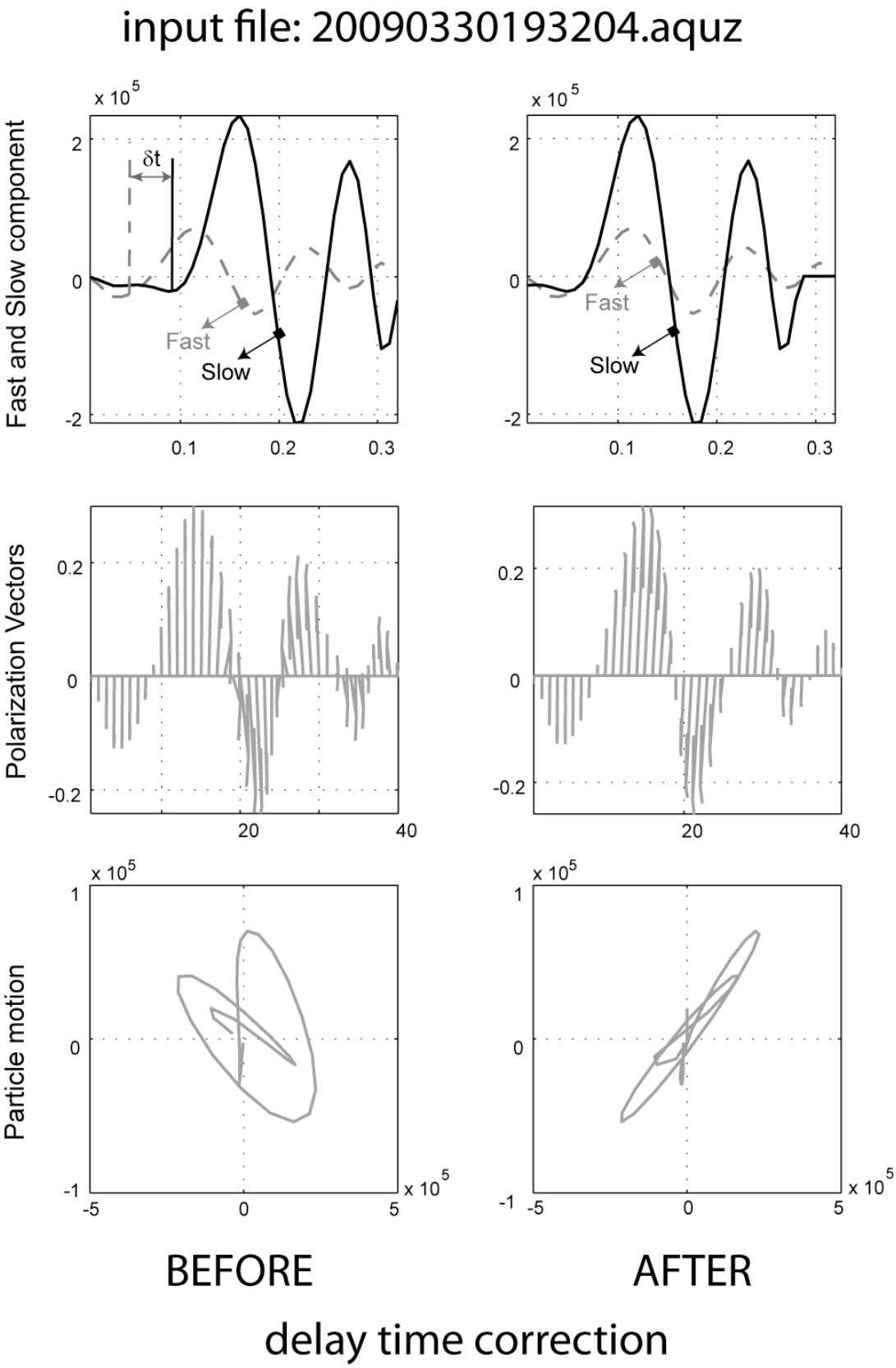
input file: 20090330193204.aquz
Fast and Slow component
Polarization Vectors
Particle motion
δt
Fast
Slow
x 10^5
BEFORE
AFTER
delay time correction

Figure 2

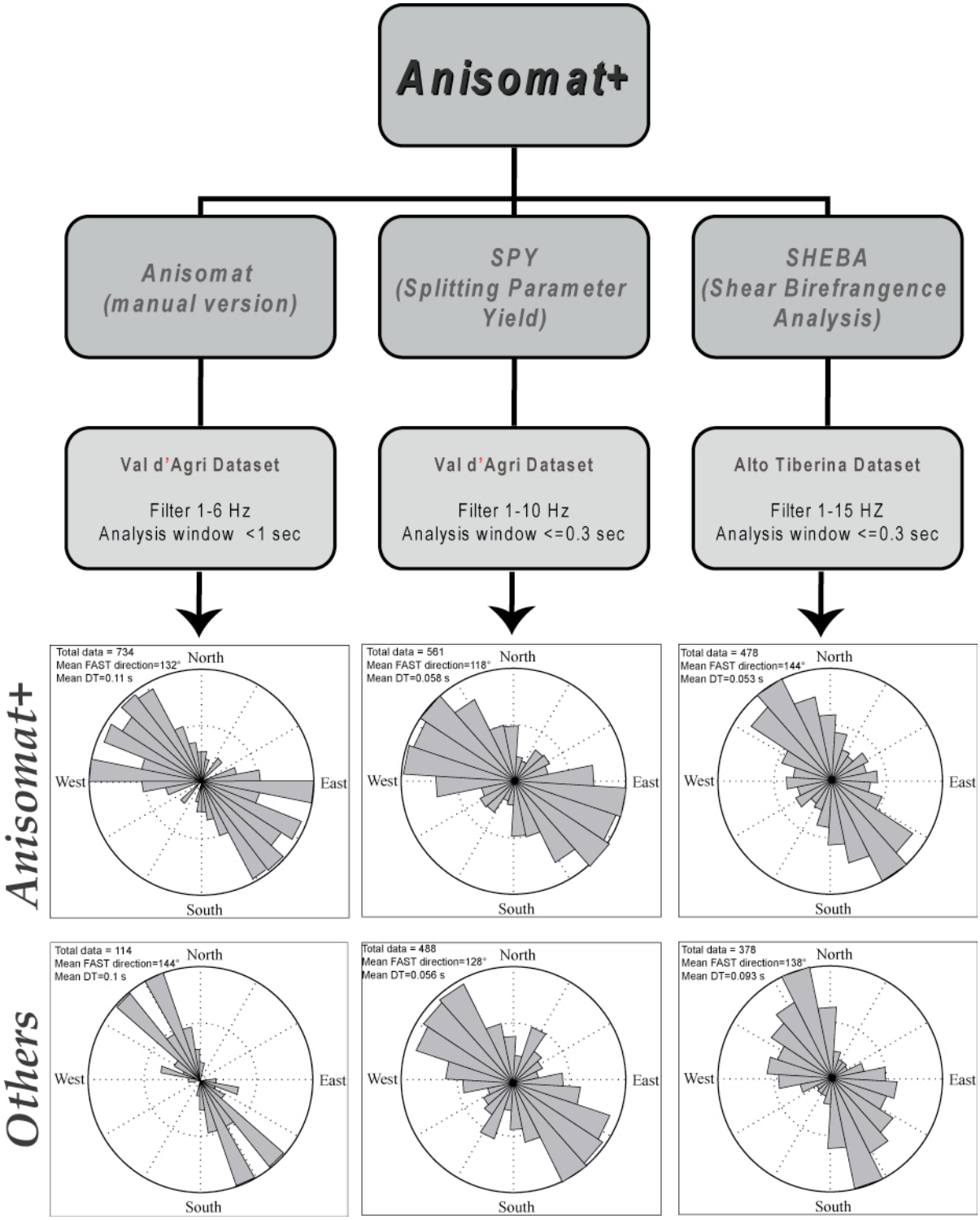
Anisomat+
Anisomat (manual version)
SPY (Splitting Parameter Yield)
SHEBA (Shear Birefrangence Analysis)
Val d'Agri Dataset
Filter 1-6 Hz
Analysis window <1 sec
Val d'Agri Dataset
Filter 1-10 Hz
Analysis window <=0.3 sec
Alto Tiberina Dataset
Filter 1-15 HZ
Analysis window <=0.3 sec
Anisomat+
Others
Total data = 734
Mean FAST direction=132°
Mean DT=0.11 s
Total data = 561
Mean FAST direction=118°
Mean DT=0.058 s
Total data = 478
Mean FAST direction=144°
Mean DT=0.053 s
Total data = 114
Mean FAST direction=144°
Mean DT=0.1 s
Total data = 488
Mean FAST direction=128°
Mean DT=0.056 s
Total data = 378
Mean FAST direction=138°
Mean DT=0.093 s
North
West
East
South

Figure 3

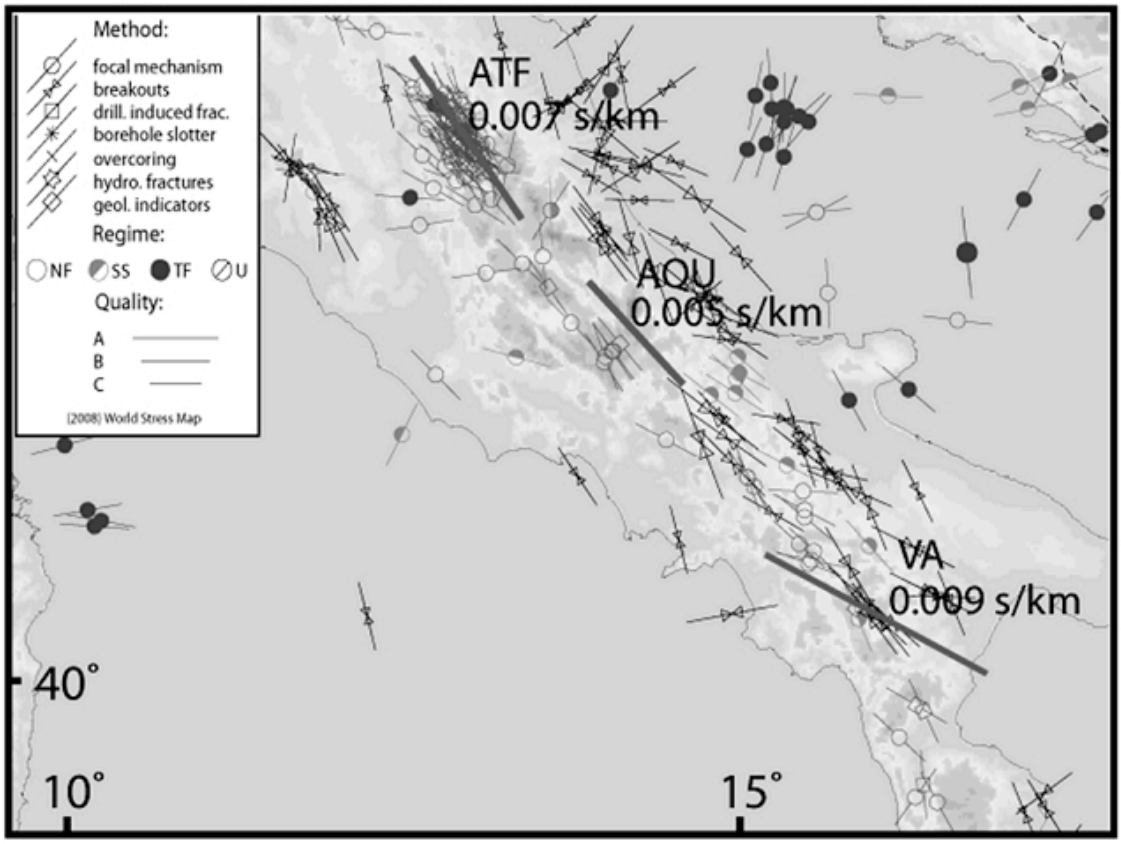
Method:
focal mechanism
breakouts
drill. induced frac.
borehole slotter
overcoring
hydro. fractures
geol. indicators
Regime:
NF
SS
TF
U
Quality:
A
B
C
(2008) World Stress Map
ATF
0.007 s/km
AQU
0.005 s/km
VA
0.009 s/km
40°
10°
15°

Figure 4

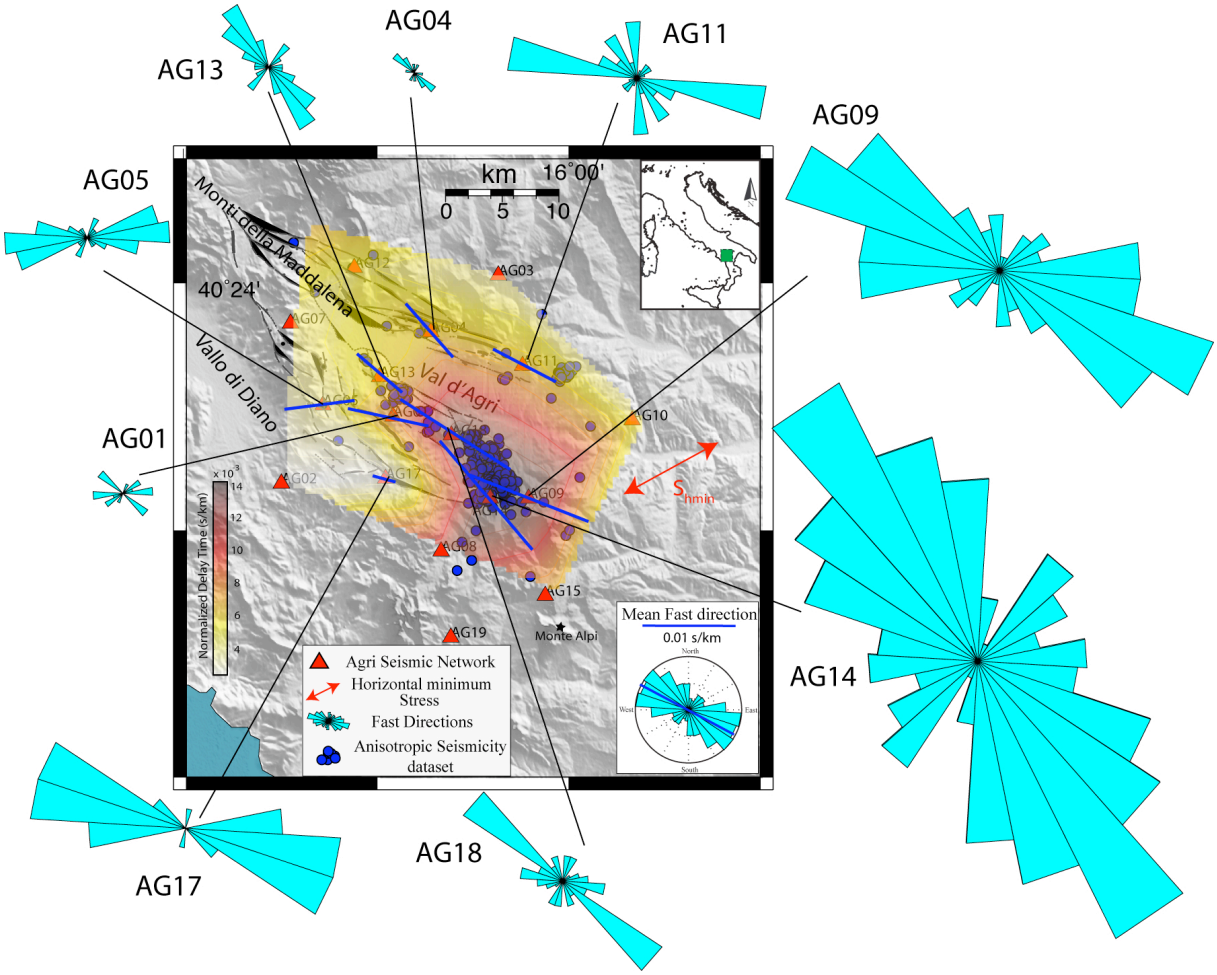
AG04
AG11
AG13
AG09
AG05
AG01
AG14
AG17
AG18
km
0 5 10
16°00'
40°24'
Monti della Maddalena
Vallo di Diano
Val d'Agri
AG03
AG07
AG12
AG13
AG11
AG10
AG02
AG17
AG09
AG08
AG15
AG19
Monte Alpi
Shmin
x 10^3
Normalized Delay Time (s/km)
14
12
10
8
6
4
Agri Seismic Network
Horizontal minimum Stress
Fast Directions
Anisotropic Seismicity dataset
Mean Fast direction
0.01 s/km
North
West
East
South

Figure 5

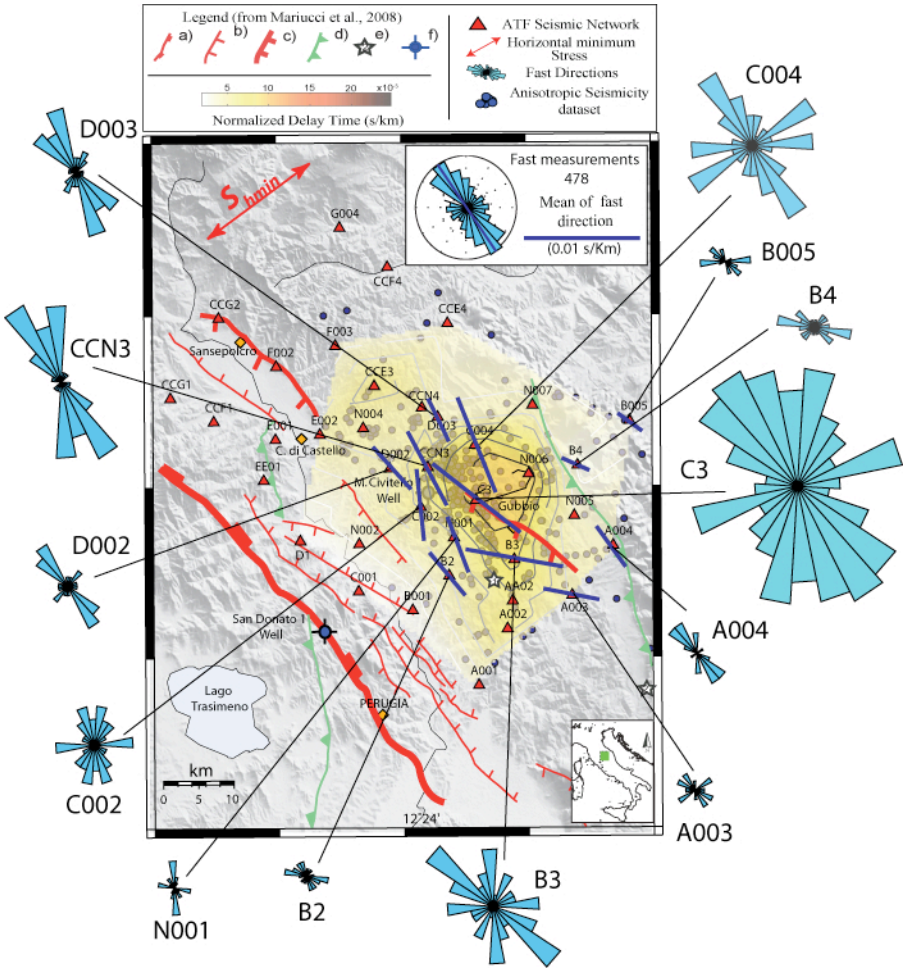
Legend (from Mariucci et al., 2008)
a)
b)
c)
d)
e)
f)
5
10
15
20
x10⁻⁵
Normalized Delay Time (s/km)
ATF Seismic Network
Horizontal minimum Stress
Fast Directions
Anisotropic Seismicity dataset
Fast measurements
478
Mean of fast direction
(0.01 s/Km)
S hmin
G004
CCF4
CCE4
CCG2
F003
Sansepolcro
F002
CCE3
CCG1
CCF1
CCN4
N004
N007
B005
E001
E002
D003
G004
C. di Castello
F002
CN3
N006
B4
EE01
M. Civitello Well
C3
Gubbio
N005
C002
F001
N002
A004
P1
B3
B2
C001
AA02
B001
A002
A003
San Donato 1 Well
A001
Lago Trasimeno
PERUGIA
km
0
5
10
12°24'
D003
C004
B005
B4
CCN3
C3
D002
A004
C002
A003
N001
B2
B3

Figure 6

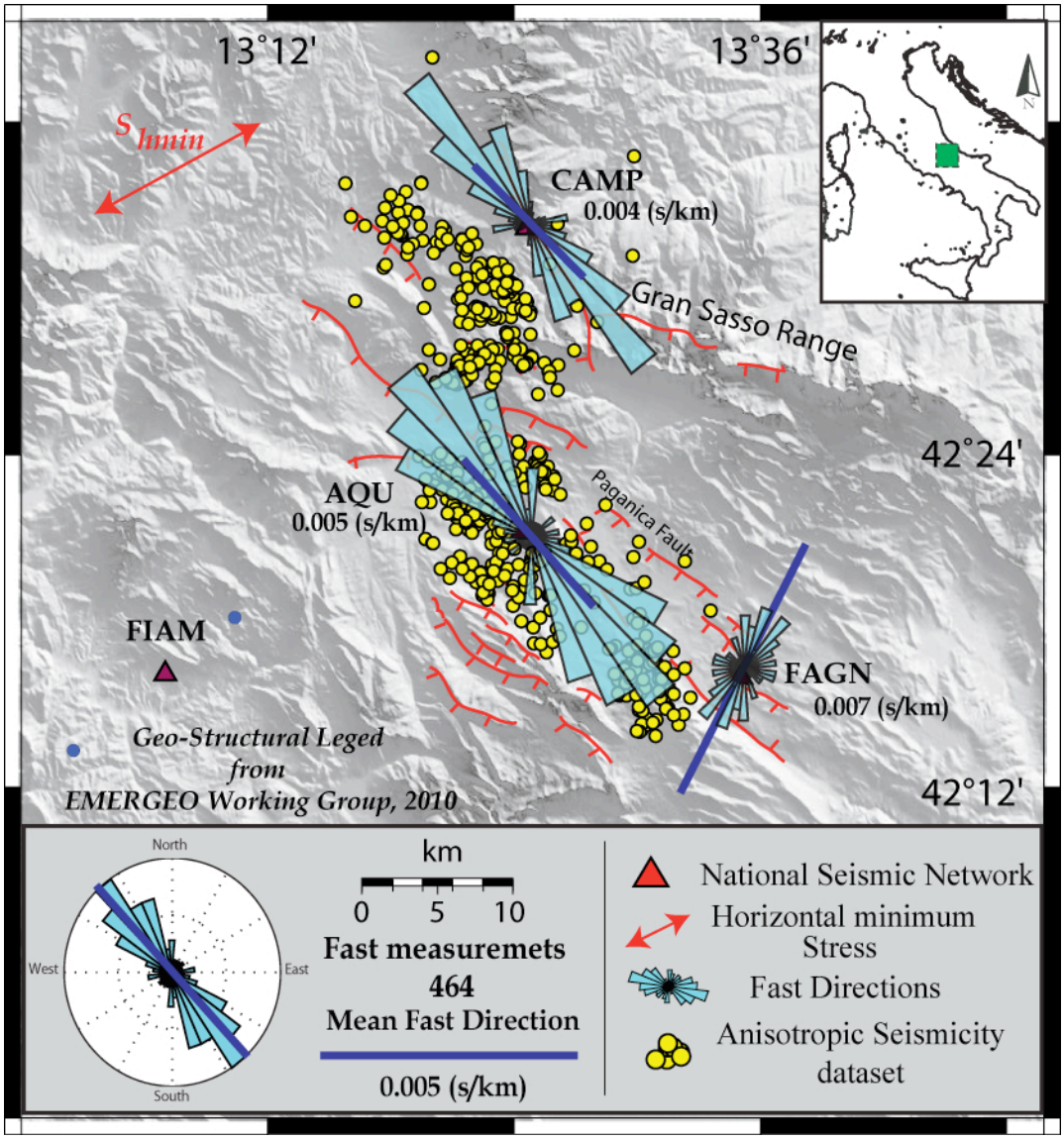
13°12'
13°36'
42°24'
42°12'
S hmin
CAMP
0.004 (s/km)
Gran Sasso Range
AQU
0.005 (s/km)
Paganica Fault
FIAM
FAGN
0.007 (s/km)
Geo-Structural Leged
from
EMERGEO Working Group, 2010
North
West
East
South
km
0 5 10
Fast measuremets
464
Mean Fast Direction
0.005 (s/km)
National Seismic Network
Horizontal minimum Stress
Fast Directions
Anisotropic Seismicity dataset

Figure 7

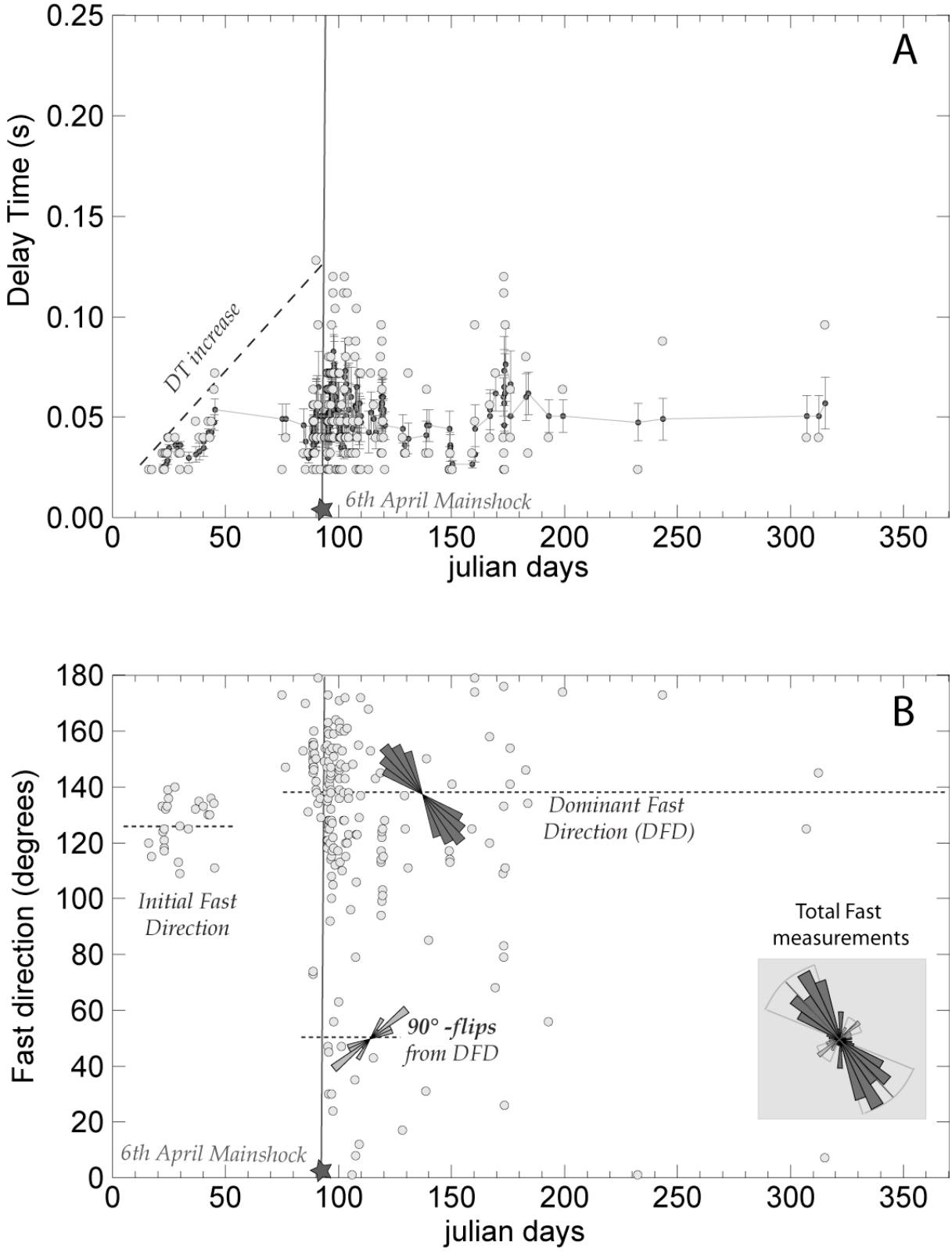
A
Delay Time (s)
0.25
0.20
0.15
0.10
0.05
0.00
DT increase
6th April Mainshock
0
50
100
150
200
250
300
350
julian days
B
Fast direction (degrees)
180
160
140
120
100
80
60
40
20
0
Dominant Fast
Direction (DFD)
Initial Fast
Direction
Total Fast
measurements
90° -flips
from DFD
6th April Mainshock
julian days

Figure 8